



PERFORMANCE OF COLUMNS WITH SHORT LAP SPLICES

Murat MELEK¹ and John W. WALLACE²

SUMMARY

Splices in reinforced concrete columns of older buildings were commonly designed as compression lap splices, which are typically only 20 to 24 bar diameters (d_b) long and enclosed within light transverse reinforcement. Observations of column damage following earthquakes have revealed that these splices perform poorly; however, relatively sparse information exists to assess the expected splice performance which hinders the development of efficient and cost-effective rehabilitation strategies. A research program was undertaken to subject full-scale, cantilever columns with lap splices to constant axial load and reversed cyclic lateral displacements applied at the top of the column. Primary test variables included the level of axial load, the moment-to-shear ratio, and the loading history. Test results indicate that envelop lateral load versus lateral drift relations were quite insensitive to changes in axial load and shear demands less than V_n . However, the post-peak strength degradation was most sensitive to the loading history.

INTRODUCTION

Code provisions for lap splices of column longitudinal reinforcement for special moment frames have undergone significant revisions since the late 1950s. In the 1956 ACI code [1], a minimum lap splice length of $20d_b$ was specified. Splice lengths were increased to $24d_b$ for compression and to $36d_b$ for tension for Grade 60 column bars in the 1963 ACI code [1]. A minimum compression lap length of $30d_b$ was specified in ACI 318-77 [1]; however, by the 1983 code [1], requirements dictated that column compression lap splices be proportioned as tension splices and located within the center half of the column. In the 1989 code [1], requirements for moderate amounts of transverse reinforcement over the entire column height were added, whereas in 1999 [1], more stringent requirements for transverse reinforcement along the lap length were added.

Given the code requirements for pre-1977 buildings, many buildings exist where splices of column longitudinal reinforcement were designed for compression only, typically with lap lengths of $20d_b$ and $24d_b$ and with relatively light transverse reinforcement enclosing the lap. Under earthquake actions, the

¹ Graduate Research Assistant, Dept. of Civil and Environmental Engineering, University of California, Los Angeles, CA 90095-1593

² Associate Professor, Dept. of Civil and Environmental Engineering, University of California, Los Angeles, CA 90095-1593

column typically develops significant moments subjecting the longitudinal reinforcement within the splice region to tensile stresses, particularly if the splice is located just above the floor slab, which is common in older construction. Given that required lap lengths for tension substantially exceed those for compression, slip along the splice length at load levels less than that required to reach the nominal moment capacity of the column may occur, resulting in loss in column strength and stiffness. The load-deformation responses of columns representative of those found in older buildings are not well understood, and in particular, the degradation of strength and stiffness and the ability of the column to resist axial load after loss of lateral load capacity are of interest.

In addition to splices in older buildings, performance of splices in so-called non-participating elements is of interest (see “Uniform”, 1994, Section 1631.2.4 and 1997, Section 1633.2.4) [2]. Deformation compatibility requirements govern the design of splices for columns not designed to be part of the lateral-force-resisting system. Following damage observed in the 1994 Northridge earthquake, more stringent requirements for transverse reinforcement for these non-participating columns were incorporated within ACI 318-95 [1], and subsequently into UBC-97 [2]. The need for these new provisions indicates that substandard lap-splices (and shear reinforcement) may exist even in relatively recent building construction (e.g., pre-1995).

PRIOR EXPERIMENTAL STUDIES

Studies of lap-splice behavior for cyclic loads date from the 1970s, with initial efforts focused on determining development length requirements for code provisions, followed by studies to address rehabilitation needs. Relatively little research has been conducted to assess the behavior of columns with deficient lap splices as early work focused primarily on developing rehabilitation options for splices (e.g., Aboutaha et al. [3], Chai et al. [4] and Valluvan et al.[5]). A majority of the available information on the behavior of columns with substandard lap-splices subjected to cyclic loading is gleaned from these experimental studies, as it was common practice to use a reference column (no rehabilitation) to assess the effectiveness of various rehabilitation strategies. Reference specimens tested in these studies had splice lengths of $20d_b$ for Grade 40 bars [3, 4] and $24d_b$ for Grade 60 bars [5]. The experiments revealed that reference specimens with $20d_b$ lap splice lengths experienced bond deterioration prior to reaching the nominal moment capacity at the critical section. Evaluation of the test results produced by Aboutaha [3] and Chai [4] indicate that using a steel jacket is an effective method for improving the cyclic response of the columns with compression lap splices. Even damaged specimens, once repaired with steel jackets, showed ductile behavior [4]. The reference (no rehabilitation) specimen tested by Valluvan [5] also exhibited poor performance under cyclic loading, with a sudden loss in lateral load capacity at approximately two-thirds of the nominal tensile capacity of the longitudinal reinforcement. Rehabilitation measures, such as the use of steel angles and straps or ties with grout and welding the lap spliced bars, improved the performance of the specimens.

Lynn et al. [6] investigated the behavior of columns with pre-1970s construction details by testing eight, 457.2 mm (18 in.) square columns with Grade 40 ($f_y = 275$ MPa) 25.4 mm (#8) or 32.3 mm (#10) longitudinal reinforcement bars. Three specimens out of eight were provided with splices ($20d_b$ and $25d_b$) at the base of the columns. The specimens were subjected to reversed cyclic lateral displacements as a function of calculated yield displacement while the axial stress was held constant for the duration of the test at either $0.12f'_c$ or $0.35f'_c$.

All specimens failed in shear, although specimens with low axial load ($0.12A_gf'_c$) and longitudinal steel ratio (2%) showed fairly ductile response (displacement ductility of 4.2 and 3.5, respectively) compared with other specimens. Although the yield stress was reached in the spliced bars, cracks along the lap

splice led to strength degradation and eventually shear failure (just above the splice) in the specimens with low axial stress. For the specimens with high axial stress, abrupt shear failures were observed for columns with and without the lap splices, shortly after reaching the bar yield stress in tension; therefore, the splice did not substantially influence the observed behavior.

SEISMIC REHABILITATION

The experimental studies briefly summarized herein mainly focused on identifying effective rehabilitation measures used for columns with inadequate lap splice lengths. Among the rehabilitation options explored, adding external ties/hoops or using steel jackets were the most effective in improving column behavior. For older buildings (e.g., pre-1977), deficient column splices are likely to exist at numerous locations both in plan and over the height of a building. Although acceptable splice performance can be achieved with a variety of rehabilitation options as noted previously, often it is not economical or practical to rehabilitate column splices in buildings given constraints on disruption or displacement of building occupants. To address these issues, a common rehabilitation strategy employed is to limit the drift imposed on “deficient” columns by adding bracing, shear walls, or a protective system (e.g., isolators, dampers) to the building such that the lateral deformations imposed on the deficient elements of the building are reduced to an acceptable level. By limiting the building lateral deformations, the forces imposed on column splices can be limited such that the spliced reinforcement does not reach a point where the splice strength begins to degrade. Rehabilitation guidelines [7] have been developed that are used by the engineering profession to accomplish this task for existing buildings. Application of the “Guidelines” [7] requires that the force versus deformation behavior of columns with short splice lengths be well characterized to allow for design of reliable and economical rehabilitation measures. Available information is limited, with the limited tests conducted by Lynn et al. [6] providing the bulk of the information.

RESEARCH SIGNIFICANCE

Sparse data exist on the performance of columns with “deficient” lap splices. This lack of knowledge on how the lateral-load behavior of column splices is influenced by important parameters such as axial load, shear, and load history leads to considerable uncertainty for seismic rehabilitation, and ultimately, conservative and costly rehabilitation measures. Given this need, a research project was undertaken to provide vital data on the performance of column lap splices for a variety of conditions. The project was part of a coordinated research project undertaken by the PEER Center to study the behaviour of older reinforced concrete frame structures.

EXPERIMENTAL RESEARCH PROGRAM

The primary focus of the research program was to produce and document experimental data on the behavior of full-scale columns with lap splices subjected to axial load and cyclic lateral load. The test specimens consisted of cantilever columns with a foundation block attached to a strong floor (Fig. 1). The specimens represent an interior building column from column mid-height between floors to the column-joint interface. A column height of between 1.52 and 1.83 meters and a 457 mm square cross section were used for the test columns. Column reinforcing details (Fig. 2), with 8 – 25.4 mm nominal diameter vertical bars and 9.5 mm diameter hoops with 90-degree hooks spaced at 304.8 mm on center along the column height, were based on a review of typical reinforcing details in older buildings, and are very similar to the details used in the specimens tested by Lynn [6].

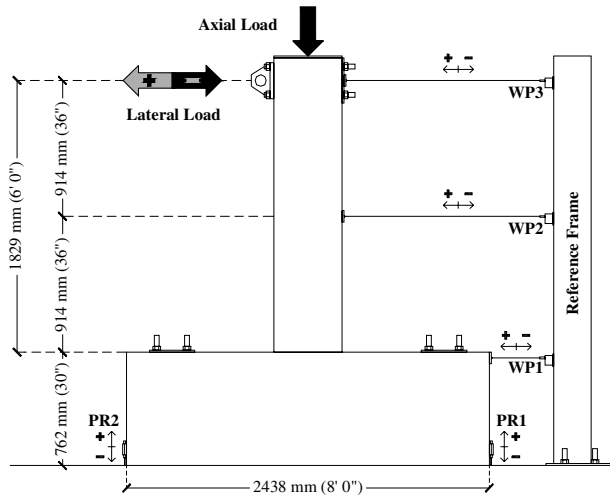


Fig. 1(a) Test setup schematic



Fig. 1(b) Test setup photo

The column height was selected to ensure the shear strength of the column using ACI 318-02 Eq. 11-4 and 11-15 was sufficient to develop the flexural strength at the base of the column, where the lap splice was located. This was done to ensure that splice failures would result, versus column shear failures, which were being studied in a companion project [8]. A lap splice length of $20d_b$ was used and axial load was applied and held constant prior to applying the uniaxial lateral displacement history at the top of the column. Anchorage at the column base was provided by a large foundation block, versus a beam-to-column connection, as the focus of the study was on splice behavior. The behavior of the beam-column joint region was the focus of another companion study [9].

A fairly typical lateral displacement history consisting of three cycles at monotonically increasing drift levels (0.1, 0.25, 0.5, 0.75, 1.0, 1.5, 2.0, 3, 5, 7, and 10%), as shown in Fig. 3, was used for five of the six specimens. A load history representative of what might be expected in the near-fault region also was used for one specimen (Fig. 3). One objective of the test program was to apply large displacement amplitudes to assess both loss of lateral load capacity and loss of axial load carrying capacity, which is important for evaluating life-safety and collapse prevention performance levels.

The primary test variables were the axial load level ($0.1, 0.2$ and $0.3A_gf'_c$), the column shear demand at maximum base moment (0.67 to $0.93 V_n$), and the applied displacement history (Table 1). The first three specimens were subjected to the standard cyclic lateral load history (STD) with the axial load held constant for the duration of the tests at $0.1, 0.2$, and $0.3A_gf'_c$ (534, 1068 and 1601 kN). A comparison of the provided lap-splice length ($20d_b$) with the lap-splice length required by ACI 318-02 (Table 1) revealed

Table 1 - Test Matrix

SPECIMEN	P % $A_gf'_c$	$\frac{l_{s_provided}}{l_{s_required}}$ *	V_c (kN)	V_n (kN)	$\frac{V_u @ M_{EXP}}{V_n}$	Column Height (mm)	Disp. History
2S10M	10	0.65	212	301	0.67	1829	STD
2S20M	20	0.65	245	334	0.70	1829	STD
2S30M	30	0.65	278	367	0.78	1829	STD
2S20H	20	0.64	242	331	0.81	1676	STD
2S20HN	20	0.64	242	331	0.81	1676	Near F.
2S30X	30	0.64	275	363	0.93	1524	STD

* ACI 318-02 Equation (12-1)

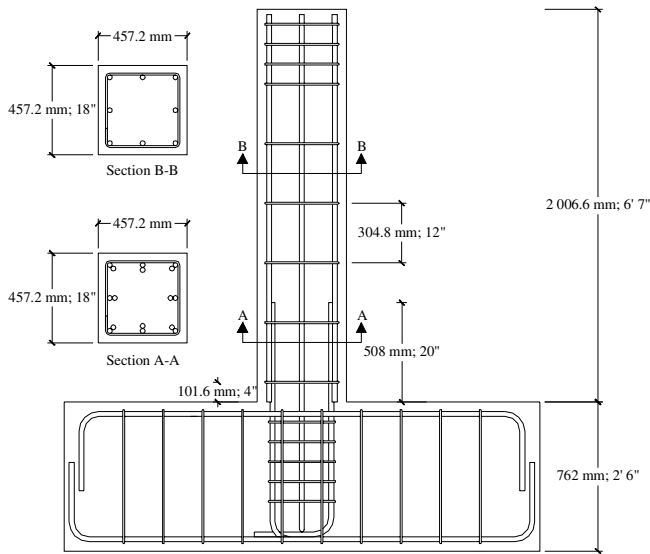


Figure 2 - Reinforcing Details

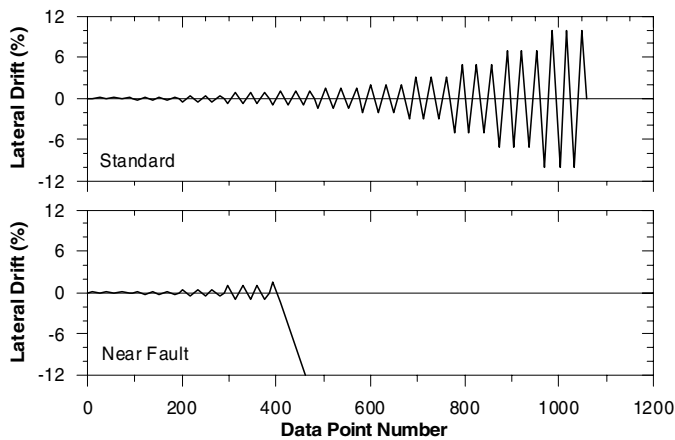


Figure 3 - Displacement Histories

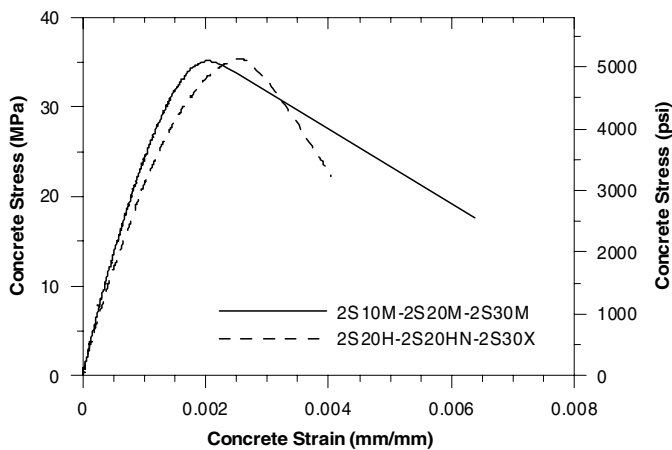


Figure 4 - Concrete Stress-Strain Relationship

that splice failure (degradation of lateral load capacity) was expected when the moment in the column reached approximately 60 to 70% of the nominal moment capacity; although a review of test data (e.g., Lynn et al. [6]) suggested that column longitudinal reinforcement might reach yield in tension. The objective of the three tests was to assess the influence of axial load on lap splices with moderate shear stress and light transverse reinforcement.

Two additional specimens were tested to investigate the influence of higher shear force and applied displacement history on column behavior for moderate axial load ($0.20A_g f'_c$). Axial load and shear were increased for the final specimen to increase the shear expected during the test to approximately the calculated nominal shear capacity (Table 1).

The specimen identification (ID) labels used are similar to those used by Lynn [6], and define the longitudinal steel ratio, the level of the applied axial load, the shear demand level at the lateral load expected to result in splice deterioration (Moderate, High and MaXimum), and the applied lateral displacement history. For example, label 2S20HN corresponds to: 2 = 2% longitudinal steel ratio (8-#8); S = Spliced; 20 = $0.20A_g f'_c$; H = High Shear Demand; N = Near Fault Lateral Displacement History.

MATERIAL PROPERTIES

Properties of the concrete and rebar used for the specimens are summarized in Table 2. Yield stress for the column vertical bars was approximately 510 MPa (74 ksi) and concrete peak stress was approximately 36 MPa (5.2 ksi) with a strain at peak stress of 0.002 and 0.0025 for the first and second concrete batches of three specimens (Fig. 4). Stress versus strain relations for the vertical reinforcing bars were not obtained because bar

Table 2 – Material Properties

Material	2S10M-2S20M-2S30M			2S20H-2S20HN-2S30X			
	f'_c (MPa)	f_{ct} (MPa)	f_r (MPa)	f'_c (MPa)	f_{ct} (MPa)	f_r (MPa)	
Concrete	36	3.4	3.8	35	-	3.7	
Steel	d_b (mm)	f_y (MPa)	f_u (MPa)	d_b (mm)	f_y (MPa)	f_u (MPa)	
	(Column)	25.4	510	818	25.4	510	818
	(Starter)	25.4	521	746	25.4	507	807
	(Ties)	9.5	481	750	9.5	481	750

yielding was not anticipated (due to the inadequate splice lengths provided). It is noted that Grade 60 longitudinal reinforcement was used for the specimens, although Grade 40 reinforcement is fairly common in older buildings, because of the difficulty (cost) associated with obtaining Grade 40 reinforcement. However, the use of Grade 60 reinforcement and a short lap-splice length ($20d_b$) ensured that splice failure would result. The results are representative of those expected for older columns as long as the deformations on the reinforcement of the existing building are consistent with those of the test columns.

TEST RESULTS

Results obtained from the experimental phase of the research program are summarized in the following subsections. Results presented include: (1) progression of damage during the tests, (2) load and moment versus lateral displacement histories, (3) moment versus slip relations, and (4) implied bond stresses. The results are used to assess the importance of the test variables on rehabilitation strategies for structural systems that include columns with short lap splices.

Observed Damage

Damage trends are presented for two specimens, 2S20M and 2S20HN to provide an overview of the type and progression of column damage at various stages of the testing. Similar trends were noted for all specimens subjected to the “standard” displacement history. Additional information is available in the report by Melek et al. (2003) [10].

2S20M: Flexural cracking first appeared at the base of the column during the first cycle of 0.25% lateral drift ratio. At a lateral drift ratio of 0.75% ($\Delta/\Delta_y=1.17$, where Δ_y is the calculated yield displacement neglecting the potential splice failure and effect of bond slip), flexural cracks developed to the height of 864 mm (47% of the column height) above the pedestal-column interface. Small longitudinal cracks along the splice length appeared during the first cycles to a peak drift level of 0.75% between the column-pedestal interface at the NW and NE corners of the column and first flexural crack above the pedestal located approximately 100 mm ($4d_b$) above the interface. During the first cycle of 1.0% drift level ($\Delta/\Delta_y=1.57$), sudden and substantial crack propagation was observed along the entire splice length (508 mm or $20d_b$) at NE corner of the column. Lateral strength degradation due to splice failure initiated during the first cycle to 1.0% drift ratio for the negative direction and during the first cycle of 1.5% drift ratio for positive direction. At 1.0% lateral drift, when lateral strength degradation initiated, longitudinal cracks were observed only at the southwest and northeast corners of the specimen. Cracks were narrow and had lengths of 114 mm ($4.5d_b$) on west face and 514 mm ($20.25d_b$) on north-east corner, at the completion of the 1% cycles ($\Delta/\Delta_y=1.57$). Bond deterioration was evident for all the longitudinal bars located on the east and west column faces. Initial hairline shear (diagonal) cracks were observed on the north and south column faces during the first cycle of 0.75% drift level. Additional shear cracks formed during the first cycle to 1.5% ($\Delta/\Delta_y=2.35$) lateral drift ratio; however, after lateral strength degradation initiated, no new

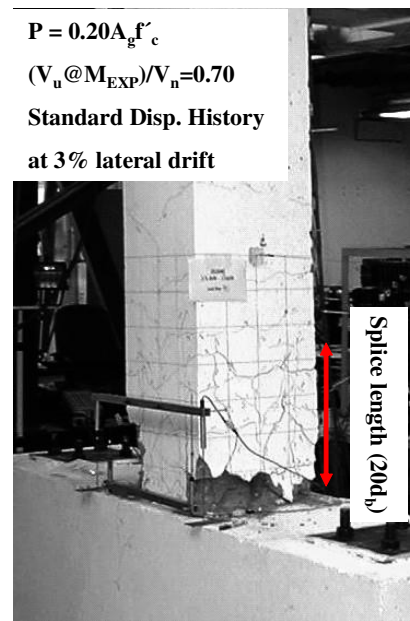
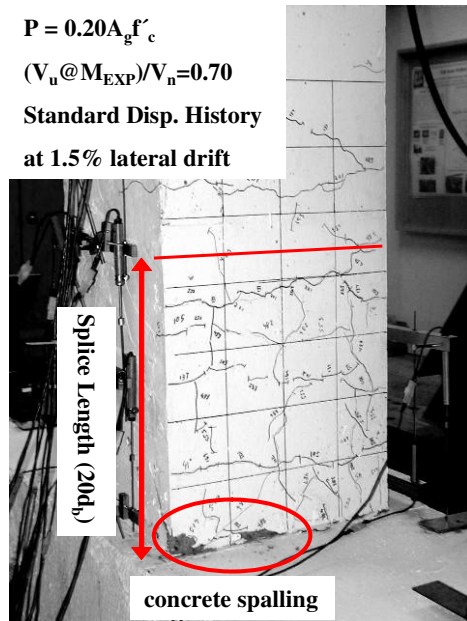


Figure 5 (left) – 2S20M concrete spalling at 1.5% lateral drift (W face)

Figure 6 (right) – 2S20M at 3% lateral drift (S-E Face)

diagonal cracks were observed. Concrete crushing and minor spalling (Fig. 5) were observed adjacent to the column-pedestal interface during the third cycle to 1.5% lateral drift ratio. After the first cycle of 3.0% ($\Delta/\Delta_y=4.70$) lateral drift was completed, all concrete cover on the east and west faces had spalled-off over the bottom 127 mm ($5d_b$) of the column and the longitudinal bars located at the southwest corner of the column were visible (Fig. 6). Once cover was lost, hoops with 90 degree bends opened, allowing vertical bars to buckle, eventually leading to loss of axial load capacity at 7% lateral drift ($\Delta/\Delta_y=10.96$) (Fig. 7).

2S20HN: A near-fault displacement history was developed to assess column behavior. The initial lateral displacement cycles were identical to the standard displacement history up to a drift level of 1.0% (except for the absence of the cycles to 0.75%), followed by one-half cycle to 1.5% ($\Delta/\Delta_y=2.60$), and then a monotonic push to large drift. Response of the specimen up to the 1.5% drift level was similar to that for the other specimens tested, i.e., longitudinal cracks along the splice length first appeared over a length of 100 mm ($4d_b$) at the base of the column, followed by propagation of the cracks along the entire splice length ($20d_b$) by 1.0% drift level. The near fault displacement history departed substantially for the standard displacement history after three cycles of 1.0% lateral drift were applied to the column. At 2% lateral drift ($\Delta/\Delta_y=3.47$), damage consisted of significant longitudinal cracking along splice length, flexural cracking over 61% of the column height and concrete crushing, which was noticeably less than observed for columns subjected to the standard displacement history. When 4.0% lateral drift ($\Delta/\Delta_y=6.94$) was reached, longitudinal crack propagation had ceased and crack widths were as wide as 4 mm. For higher drift ratios, the crack at column-pedestal interface increased substantially due to the slip of longitudinal bars relative to the starter bars anchored into the pedestal. Concrete spalling started around 4.0% lateral drift; however, it was not significant compared with the other specimens. Axial load capacity was maintained throughout the test (Figure 8).

The ability of the columns to maintain the axial load-carrying capacity during the experiment was an important consideration during testing. The applied axial load was continuously monitored and held constant throughout the duration of each experiment. Two of the five specimens: 2S10M and 2S20HN were able to carry the applied axial load to the maximum lateral drift that could be applied by the actuator (10% for 2S10M, and 12% for 2S20HN). After completion of the lateral displacement history, the lateral

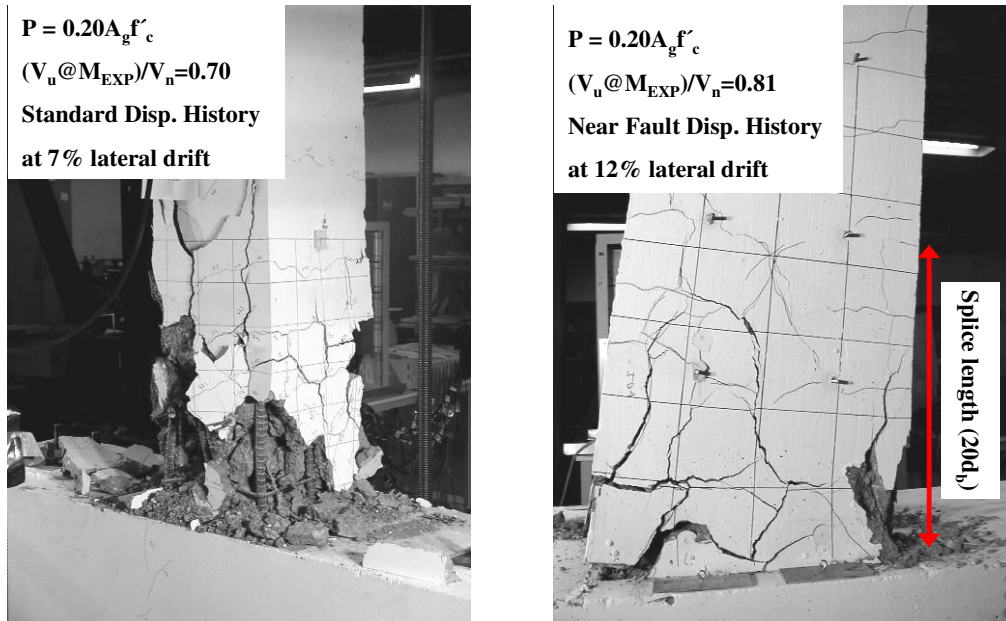


Figure 7 (left) – 2S20M at 7% lateral drift after loss of axial load capacity (N-W Face)
Figure 8 (right) – 2S20HN at 12% lateral drift (N face)

drift applied to specimen 2S10M was returned to zero, and the axial load was monotonically increased until failure, which occurred when an axial load of $0.20A_g f'_c$ was reached. Unlike specimens 2S10M and 2S20HN, specimens 2S20M, 2S30M, 2S20H, and 2S30X lost axial load-carrying capacity during the test. Specimens with moderate and high axial load reached 7% and 5% lateral drift, respectively. The axial load-carrying capacity generally began to degrade when hoops at the 101.6 mm and 406.4 mm levels above the pedestal opened allowing the vertical bars to buckle. The hoops were fabricated with only 90° hooks, as is common with older construction, and these hooks provided little lateral support to suppress buckling once the concrete cover was lost.

The test results indicate that columns that experience lateral strength degradation due to splice failure can support significant vertical loads to large lateral displacements. The ability of the columns to maintain axial load carry capacity depends on existence of other structural elements providing sufficient lateral stability to the overall structural system. The ability of a column to support vertical loads also may be impacted by column shear or beam-to-column connection (joint) failures, which were not addressed in this study. Axial load failures for columns failing in shear were addressed in a companion study by Elwood [11]. At interior connections where beams frame into all four sides of a joint, joint failure is unlikely; however, for exterior connections, joint failures have been observed. Examples include the failures observed in the Cypress Viaduct structure during the 1989 Loma Prieta earthquake [12], and failures observed in the Kaiser-Permanente Building following the Northridge earthquake [13].

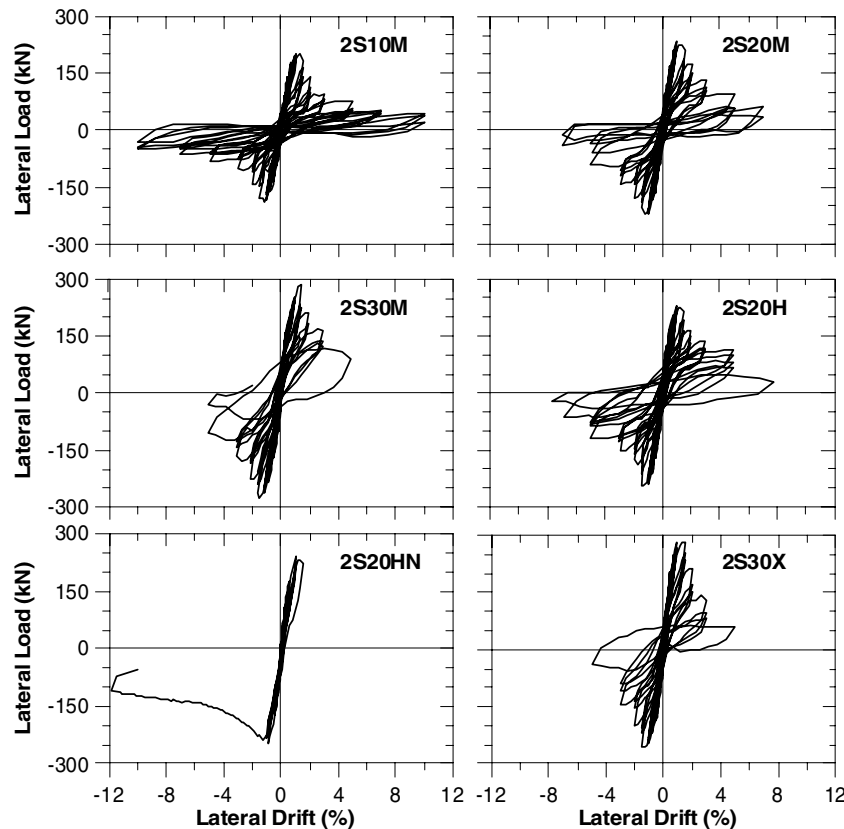
Measured responses

Lateral load versus top displacement relations, modified to eliminate the external factors such as the displacement of the reaction frame, displacement and rotation of the pedestal, and the influence of the applied axial load at the top of the column on the column shear and moment at the base of the column (P- Δ effects and effect of horizontal component of the axial loading at higher drift levels), were derived for all six specimens. The corrected and normalized lateral load – top displacement relations are plotted in Fig. 9. Measured lateral loads shown in this figure were normalized to the column height of first three specimens (1829 mm) for comparison (Table 3, Columns 2 and 4). All specimens exhibit similar responses, with sudden lateral strength degradation observed at drift levels between 1% and 1.5% ($\Delta/\Delta_y \approx$

1.5 to 2.5). Lateral strength degradation started just prior to, or just after reaching, yielding of the longitudinal starter bars. Responses are characterized as non-ductile, that is, no displacement ductility was observed and the specimens displayed limited ability to dissipate energy. The peak lateral strength reached for each specimen was influenced by the level of the applied axial load, with increased lateral load capacity with increased axial load.

An elastic perfectly plastic (EPP) model was used to normalize and compare the energy dissipation capacities of the specimens. Using lateral load versus top displacement responses, the amount of total energy dissipated by the specimen and the EPP model are calculated by finding the area bounded by the load-displacement relations. At the end of the 2% and 5% lateral drift cycles ($\Delta/\Delta_y \approx 3$ and 12, respectively), the total energy dissipated by the specimens subjected to the standard displacement history was approximately 54% and 33% of that for the EPP model. In contrast, specimen 2S20HN, which was subjected to the near-fault displacement history, displayed higher energy dissipation capacity (74% of the EPP model) for both the 2% and 5% drift levels.

Lateral drift cycles exceeding 1.5% led to significant reduction of lateral strength for all specimens, with the rate of degradation influenced greatly by the applied lateral displacement history (standard versus near fault), and somewhat by the level of the applied axial load. Specimen 2S20HN, with near fault displacement history, was able to maintain 89% and 63% of the peak capacity at lateral drift ratios of 2% and 5% ($\Delta/\Delta_y = 5.20$ to 8.67), respectively, and more than 50% of its peak lateral strength at 10% lateral drift ($\Delta/\Delta_y=17.33$). However, specimens subjected to the standard cyclic lateral displacement history exhibited more significant lateral strength degradation, with residual lateral strength of not more than 73% and 36% of the peak value at 2% and 5% lateral drift ratios, respectively. These trends are evident in Fig.



10, where normalized envelope relations of moment – lateral drift response histories are compared for specimens 2S20H and 2S20M (standard) and 2S20HN (near-fault). The rate of strength degradation of the specimens with the same lateral displacement history (i.e., standard) is similar, as noted on Fig. 11 for specimens 2S10M, 2S20M and 2S30M. Residual moment capacities at large drift ($> 5\%$) are approximately 20% of the peak values, although slightly higher residual strength is noted for specimen 2S10M, with lower axial load.

Figure 9 – Lateral Load – Top Displacement Plots

Table 3 – Test Results

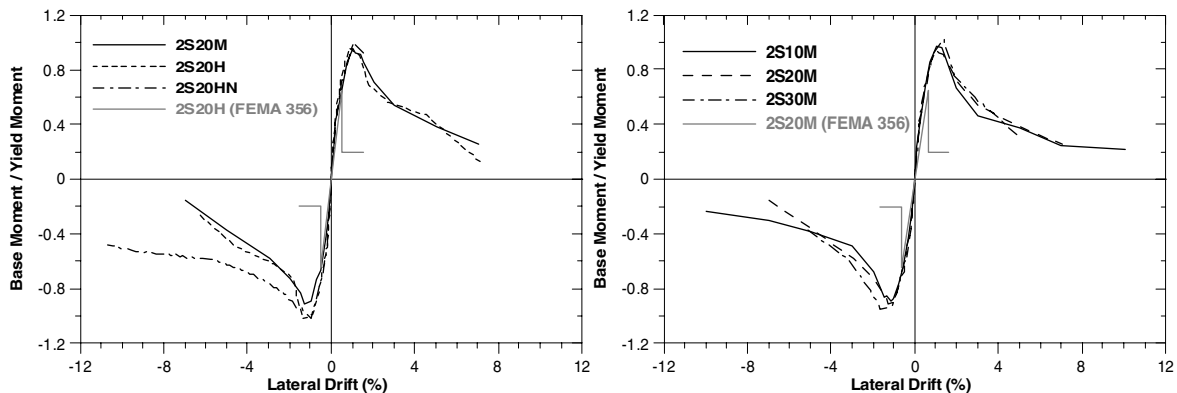
Specimen	Maximum Lateral Load		Normalized Lateral Load (kN)	Analytical Yield Moment (kN-m)	Max Base Moment M_{EXP} (kN-m)	M_{EXP}/M_y
	(kN)	@ Drift				
2S10M	202.7	1.50%	202.7	381.3	370.7	0.97
2S20M	233.5	1.28%	233.5	450.4	427.0	0.95
2S30M	285.3	1.45%	285.3	509.0	521.8	1.03
2S20H	269.5	1.33%	247.0	441.5	451.8	1.02
2S20HN	267.4	1.00%	245.1	441.5	448.3	1.02
2S30X	340.7	1.50%	283.9	499.5	519.2	1.04

* Normalized ($F_{normalized} = F_{measured} \cdot h_{column} / h_{2S10M}$)

The effect of shear demand on column response was investigated for specimens with moderate and high levels of axial load. Normalized moment versus lateral drift relations for specimens with moderate axial load (2S20M, 2S20H and 2S20HN) are compared on Fig. 10. On this plot, the yield moment values were determined by section analysis using the measured material properties. The moderate increase in shear demand from $(V_{EXP}@M_n)/V_n=0.70$ (2S20M) to 0.81 (2S20H) did not significantly impact the lateral strength or the rate of strength degradation of specimens with moderate axial load. Comparisons of results for specimens with high axial load (2S30M and 2S30X), where shear demand varied between $(V_{EXP}@M_n)/V_n=0.78$ and 0.93, reveal similar results (Table 3). The normalized moment strength M_{EXP}/M_y for the two columns with high axial load (2S30M and 2S30X) are approximately 1.03 for both cases; however, 2S30X displayed more lateral strength degradation than 2S30M after the peak lateral strength was achieved. Specimens 2S30M and 2S30X had normalized moment ratios of 0.33 and 0.23, respectively, just prior to loss of axial load capacity at 5% lateral drift.

Envelope relations used in FEMA 356 [14] also are plotted on Fig. 10 and 11. The experimental results for interior columns exhibit substantially less lateral strength degradation after bond deterioration than implied in FEMA 356.

Normalized responses of the specimens tested by Lynn [6] and Melek and Wallace with continuous and lap-spliced longitudinal reinforcement tested under low axial load ($\sim 0.10A_g f'_c$) are compared on Fig. 12. It is noted that the columns tested by Melek and Wallace (2003) were cantilever columns whereas the columns tested by Lynn [6] had double curvature with the possibility of moment redistribution. Specimen 2S10M exhibited larger deformations than the specimens tested by Lynn⁶. The level of slip at the initiation of lateral strength degradation was more significant for 2S10M than for the specimen tested by

**Figure 10 (left) – Normalized Moment – Lateral Drift 2S20M-2S20H-2S20HN****Figure 11 (right) – Normalized Moment – Drift 2S10M, 2S20M and 2S30M**

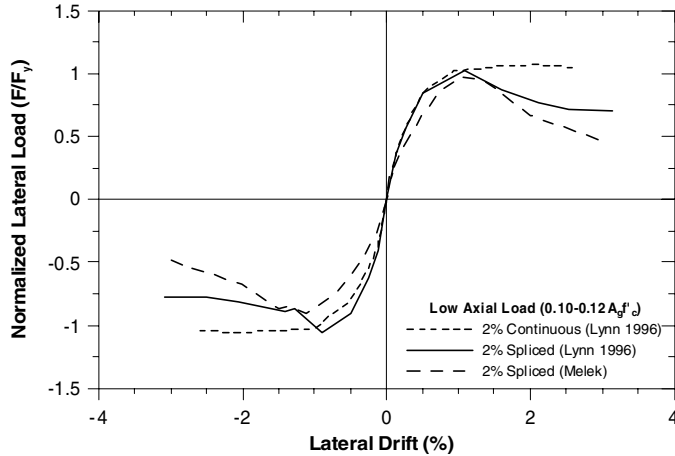


Figure 12 - Normalized Lateral Load vs. Lateral Drift Envelopes

Lynn because of higher bond stresses along the splice length due to the use of Grade 60 reinforcement for 2S10M versus with use of Grade 40 reinforcement by Lynn [6]. The impact of the inadequate splice length on lateral strength degradation is clearly seen by comparing 2S10M and specimen with continuous reinforcement and same steel ratio (Specimen 2CLH18; Lynn [6]). The specimen with continuous reinforcement was able to maintain its lateral strength up to 3% lateral drift ratio where as 2S10M lost nearly half of its lateral load capacity for the same drift level.

Moment versus slip relations

Slip along the splice can contribute significantly to column top displacement; therefore, column rigid body rotation due to slip over the splice length was characterized. These relations also are useful for calibration of moment versus slip-rotation springs that are sometimes used to model splice behavior [15]. Slip rotation was calculated by using measured displacement and strain gage data. Linear displacement transducers measured the total rotation over the splice length, whereas several strain gauges attached to the longitudinal reinforcing bars monitored the strain at several locations along the splice length. Average reinforcement strains were calculated using the strain gauge data. Slip rotation was taken as the difference between the total rotation and the rotation calculated using the average reinforcement strain along the splice length. Since measurement of slip rotation is based on strain gauge data, presented data are limited to the point where strain gauge data are collected (Fig. 13).

Column base moment and column top rotation relations (corrected) were derived to assess the contribution of slip to column top displacement. The rotation at the top of the column accounts for flexural deformations over the column height and rotations caused by slippage of reinforcement bars over the $20d_b$ splice length.

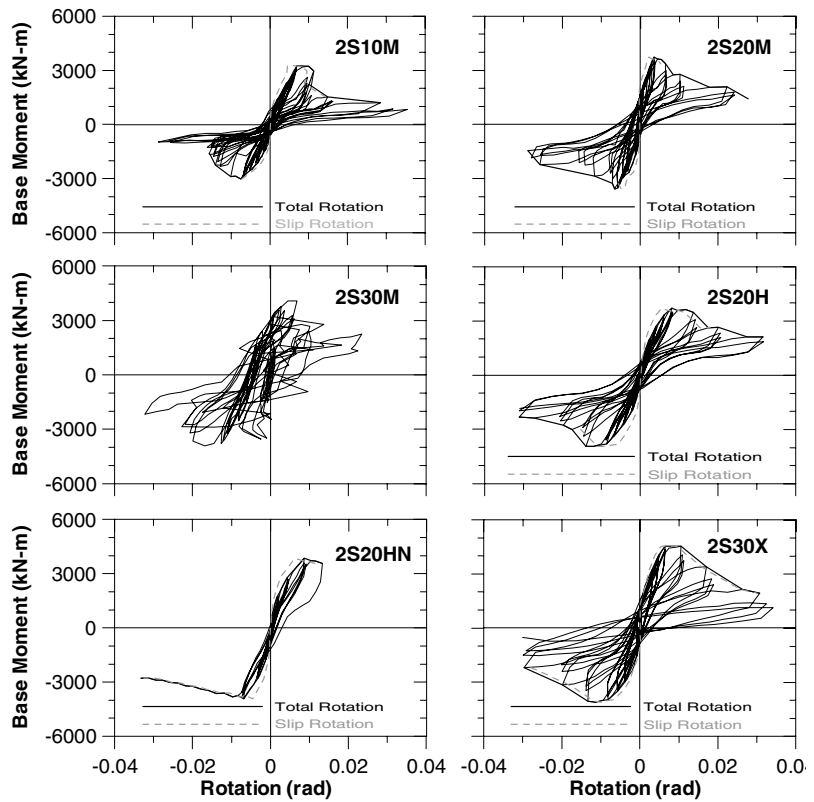


Figure 13 – Base Moment - Rotation along Splice Length Responses

Cyclic and envelope relations are presented on Fig. 16. Although no visible signs of slip were noted (e.g., vertical cracking), slip rotation constituted a significant portion of the total rotation even at the first displacement peak at 0.5% lateral drift, where ratios of slip rotation to total rotation of 50 to 75% were calculated for all specimens. When a lateral drift ratio of 1.5% was reached ($\Delta/\Delta_y \approx 2.2$ to 2.6), slip rotations accounted for 80 to 90% of top displacement for all specimens indicating substantial slip rotation prior to observed strength degradation.

Steel strain profiles

Strain histories for longitudinal column reinforcement were used to plot the strain distribution along the splice length at peak values of lateral drift, as well as to determine bond stress-slip relations needed for calibration and use of analytical models. Damage to the specimens ultimately led to failure of the strain gauges; generally at about 3% lateral drift; therefore, readings for higher drift ratios are not available for most of the strain gauges. In general, three strain gauges were affixed to the column longitudinal bars and two gauges were affixed to the starter bars anchored into the pedestal. Also, it is known that longitudinal strain is equal to zero at the ends of the longitudinal reinforcement bars. Based on the measured and known values, strain profiles were derived and plotted (Fig. 18) for specimen 2S30M. Lateral strength degradation coincided with the initiation of bond deterioration along the splice length, and bond deterioration was most significant at the lower half of the splice length, where the maximum moment occurred.

Strain profiles indicate that corner and middle longitudinal bars behave differently. For all specimens subjected to standard cyclic displacement histories, bond deterioration was first observed at the corner bar (NW) after 1.0% lateral drift ($\Delta/\Delta_y \approx 1.6$), whereas bond deterioration for the middle (W) longitudinal bar was not observed until a drift ratio of 1.5% ($\Delta/\Delta_y \approx 2.4$). This trend is especially evident for the strain distributions of the interior and exterior bars of specimen 2S30M (Fig. 14).

The average bond stress developed along the splice at peak load was calculated and compared with values typically used in design. The average bond stress (u) between reinforcing bars and the surrounding concrete was calculated using the variation of longitudinal steel strains over the splice length (determined from strain gauges). A steel modulus of 200,000 MPa (29,000 ksi) was used to transform measured steel strains (ϵ) to longitudinal steel stresses (f_s), unless bar yielding was observed, and then a bilinear steel stress – strain relation was used to obtain steel stress. Calculated longitudinal stresses were later transformed into an average bond stresses as:

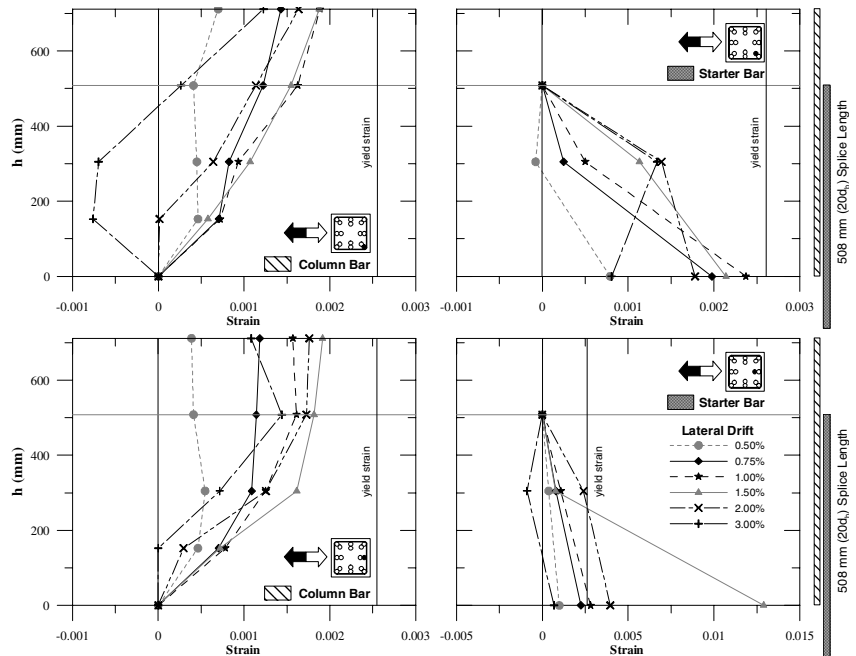


Figure 14 - 2S30M - Strain Distributions along Splice Length

$$u = \frac{f_s \cdot d_b}{4 \cdot l} \quad (1)$$

where f_s is the change in the axial stress on the bar, d_b is the nominal bar diameter and l is the length of the splice. Calculated average bond stress values (u), normalized by dividing with $\sqrt{f_c'}$, are plotted on Fig. 15.

Average bond stress implied by ACI 318-02 is obtained using equation (12-1) of ACI 318-02:

$$\frac{l_d}{d_b} = \frac{3}{40} \frac{f_y}{\sqrt{f_c'}} \frac{\alpha\beta\gamma\lambda}{\left(\frac{c + K_{tr}}{d_b}\right)} \quad (2)$$

where f_y = the measured yield stress (510 MPa), f_c' = the measured concrete strength (35.9 MPa), $\alpha\beta\gamma\lambda = 1$, $c = 2.375d_b$ for the given conditions, and K_{tr} is assumed to be zero. The resulting value from (2), $l_d/d_b=32.4$, is substituted into (1) with $f_s = f_y$ to produce an implied bond stress of $0.66\sqrt{f_c'}$ MPa ($7.9\sqrt{f_c'}$ psi). Results plotted on Fig. 19 reveal an average bond stress of approximately $0.88\sqrt{f_c'}$ MPa ($10.5\sqrt{f_c'}$ psi), with a lower bound bond stress of approximately $0.66\sqrt{f_c'}$ MPa ($8\sqrt{f_c'}$ psi). The ratio of the average bond stress derived from the column tests and that implied by ACI 318-02 is 1.33 (without applying a 1.3 reduction because all bars are spliced at one location). Given that ACI 318 significantly

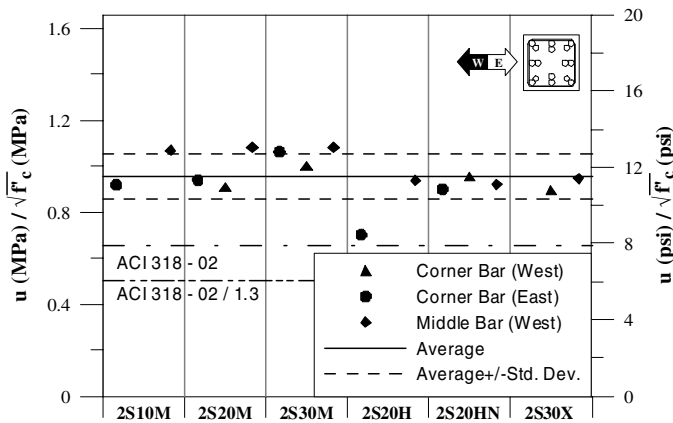


Figure 15 – Normalized measured bond strengths

underestimates the bond stresses derived from the tests (the ACI equation provides a lower bound), actual moments and shears developed in a column with splices may substantially exceed those estimated using (2), especially if an additional 1.3 factor is applied because all bars are spliced at one location. This possibility should be considered in the evaluation of older columns, as ignoring it could lead to unanticipated column shear failures (i.e., the column will develop larger moment and shear than anticipated).

CONCLUSIONS

Tests were conducted on six cantilever column specimens with $20d_b$ lap splices to assess column and splice behavior under a variety of conditions. The provided lap length is approximately 67% of what is currently required by ACI 318-02 to reach the yield stress of the reinforcement in tension. Five of the specimens were subjected to a “standard” displacement history, whereas one specimen was subjected to a “near-fault” displacement history. Based on the test results, the following conclusions are reached:

Maximum moments reached during the tests ranged from 97% to 103% of the calculated yield moments, indicating that actual bond stresses were higher than those implied by ACI 318-02. Average bond stress values from the tests were $0.88\sqrt{f_c'}$ MPa ($10.5\sqrt{f_c'}$ psi), with a standard deviation of $0.13\sqrt{f_c'}$ MPa ($1.6\sqrt{f_c'}$ psi), compared with an implied value of $0.66\sqrt{f_c'}$ MPa ($7.9\sqrt{f_c'}$ psi) from ACI 318-02. The

higher bond stresses observed relative to typical design values indicate that the potential for column shear failures might be overlooked.

Lateral strength deterioration initiated between 1.0% and 1.5% ($\Delta/\Delta_y \approx 1.6$ to 2.4, where Δ_y is calculated ignoring splice slip) lateral drift ratios for all specimens, with no observed displacement ductility for any of the specimens. Strength degradation resulted from bond deterioration between reinforcement bars and the surrounding concrete, and the rate of degradation was dependent mainly on the applied displacement history, and to a lesser degree on the level of the applied shear and the level of axial load. Significantly less strength degradation was noted for the specimen subjected to the near-fault displacement history. At 2% and 5% lateral drift ($\Delta/\Delta_y \approx 3.2$ to 8.0), the specimen subjected to the near-fault displacement history maintained 89% and 62% of peak lateral force applied, compared with average values of 73% and 36% for specimens subjected to the standard displacement history displayed ($73/89 = 82\%$; $36/63 = 57\%$).

Changes in shear strength ratios V_{EXP}/V_n , where V_n is the column shear strength computed using ACI 318-02 equation 11-4 and 11-15, between 0.67 and 0.93 did not appear to influence the lateral load at which bond deterioration initiated. However the rate of lateral strength degradation increased slightly with increasing shear level.

Plots of normalized moment (M_{EXP}/M_y) for specimens tested with 0.10, 0.20 and $0.30A_g f'_c$ (shear level between 0.67 and 0.78) indicate that variation in axial load had only a marginal impact on the lateral load at which bond deterioration initiated. As well, degradation of lateral strength was similar for all specimens. Axial load level did impact the column energy dissipation capacity modestly, with decreasing energy dissipation capacity as the axial load level was increased.

Specimens with low axial load were able to maintain the axial load carrying capacity to very high drift ratios, typically about 10% of the column height. Columns with medium and high axial load levels lost axial load carrying capacity during the cycles to 7% and 5% lateral drift, respectively. Specimens with low axial load maintained a residual axial load capacity of approximately 20% of the peak axial load capacity, with slightly lower values for columns with higher axial load. The ability of the columns to maintain axial-load carry capacity to large drift ratios despite heavy damage and significant loss of lateral-load capacity indicates that splice failures by themselves do not create a collapse hazard provided the lateral strength and stiffness of the system is sufficient to ensure lateral stability of the system. Column shear failures and joint failures, particularly at exterior connections, appear to be more likely to result in loss of axial-load carry capacity of columns; these issues were not addressed in this study.

Investigation of moment-rotation responses of the specimens indicated that rotation caused by slippage of longitudinal bars accounted for a significant portion of the total rotation. After bond deterioration initiated, rotational response was dominated by slip.

ACKNOWLEDGEMENTS

The work presented in this report was funded by Pacific Earthquake Engineering Research Center (PEER), Project #5031999. The authors would like to thank former undergraduate students Matt Brunnings, Nick Bucci, Timothy Chen, Jim Norum, Matt Pollard, Chris Petteys and Bryan Waters for their contributions to the construction, instrumentation, and testing of column specimens. Special appreciation is extended to UCLA graduate students Kutay Orakcal, Thomas Hyun-Koo Kang, Paul Ko, Leonardo Massone, Brian Sayre, and Eunjong Yu who helped at various stages of the experimental program. The authors also would like to acknowledge Dr. Thomas Sabol of Englekirk and Sabol Consulting Engineers and Ms. Brenda Guyader of Degenkolb Engineers for their contributions during the early stages of the

project. Opinions, conclusions and recommendations are those of the authors, and do not necessarily represent those of the sponsor or other individuals mentioned.

REFERENCES

1. ACI Committee 318, “*Building Code Requirements for Reinforced Concrete (ACI 318-56 63, 77, 83, 95, 99, 02)*,” American Concrete Institute, Farmington Hills, MI, 1956, 1963, 1977, 1983, 1995, 1999 and 2002.
2. Uniform Building Code, 1994 and 1997, “International Conference of Building Officials,” Whittier, CA
3. Aboutaha, R., M. D. Engelhardt., J. O. Jirsa, M. E. Kreger., (1996). “Retrofit of Concrete Columns with Inadequate Lap Splices by the Use of Rectangular Steel Jackets,” *Earthquake Spectra*, Vol. 12, No. 4, November 1996, pp. 693-714.
4. Chai, Yuk; Priestley, M.; and Seible, Frieder; "Seismic Retrofit of Circular Bridge Columns for Enhanced Flexural Performance," *ACI Structural Journal*, V88., No.5, September-October 1991, pp. 572-584.
5. Valluvan, R., M. E. Kreger, J. O. Jirsa. (1993). “Strengthening of Column Splices for Seismic Retrofit of Nonductile Reinforced Concrete Frames,” *ACI Structural Journal*, V. 90, No. 4, July-Aug. 1993, pp. 432-440.
6. Lynn, A. C., J. P. Moehle, S. A. Mahin, W. T. Holmes (1996), “Seismic Evaluation of Existing Reinforced Concrete Building Columns,” *Earthquake Spectra*, Vol. 12, No. 4, November 1996, pp. 715-739.
7. Federal Emergency Management Agency, “Guidelines for the Seismic Rehabilitation of Buildings,” *Report No. FEMA-273*, October 1997.
8. Sezen, H., J. P. Moehle (2002), “Seismic behavior of Shear-Critical Reinforced Concrete Building Columns,” Seventh U.S. National Conference on Earthquake Engineering: *Proceedings*, 2002 7NCEE, July 21-25, 2002, Boston, Massachusetts, EERI, Oakland, 2002.
9. Lehman, D. E., W. G. Mosier, J. F. Stanton (2000), “Seismic Assessment of Reinforced Concrete Beam-Column Joints”, *US-Japan Workshop on Performance-Based Seismic Design of Reinforced Concrete Buildings*, September 2000.
10. Melek, M.; J. W. Wallace; Conte J. P.(2003), “Experimental Assessment of Columns with Short Lap Splices Subjected to Cyclic Loads,” Pacific Earthquake Engineering Research Center, University of California, Berkeley, California, April 2004, 176 pages
11. Elwood, K. J. (2002), “Shake Table Tests and Analytical Studies on the Gravity Load Collapse of Reinforced Concrete Frames,” Ph.D.Thesis, University of California, Berkeley, Fall 2002.
12. The Governor’s Board of Inquiry on the 1989 Loma Prieta Earthquake (1990), “Competing Against Time: Report to Governor George Deukmejian“, May 1990, North Highlands, California, pp. 27-30
13. Earthquake Engineering Research Institute, “Northridge earthquake January 17, 1994: preliminary reconnaissance report,” Earthquake Engineering Research Inst., Oakland, California, Mar. 1994, 104 pages
14. Federal Emergency Management Agency, “Prestandard and commentary for the seismic rehabilitation of buildings,” FEMA (Series) 356, Federal Emergency Management Agency, Washington, D.C., 2000, pp.6-17 – 6-22.
15. Reyes, O.; Pincheira, J. (1999), “RC Columns with Lap Splices Subjected to Earthquakes,” *Structural Engineering in the 21st Century: Proceedings*, 1999 Structures Congress, April 18-21, 1999, New Orleans, Louisiana, ASCE, Reston, Virginia, 1999, pp. 369-372